



Semnan University

*Research Article*

# Epsilon- negative (ENG) composites characteristics at GHz frequency

Ali Bahari\*, Abbas Farhadi

Department of Solid State Physics, University of Mazandaran, Babolsar, 4741695447, Iran

**ARTICLE INFO****Article history:**

Received: 2025-12-03

Revised: 2026-01-28

Accepted: 2026-02-04

**Keywords:**

Optoelectronic device;

Lithium crystallites;

Negative permittivity;

**ABSTRACT**

Negative permittivity devices or Epsilon- negative (ENG) composites are of great importance in shielding, antennas and nano-optoelectronics applications at GHz frequencies. In recent years, many researchers have study some ferrite - based materials with metal particles for finding an alternative ENG composites in the fabrication of optoelectronic resonance components, antennas and invisible coating's industries. In the present work, an attempt has been made to investigate the optical, dielectric and electronic characteristics of the ferrite yttrium-iron-copper garnet matrix (FYICG) with different lithium (Li) nano-particles, synthesized by in situ method at 650-1250 °C and at 80- 120 GHz. The measurement cut-off frequency and modulation, sample morphology (studied with Scanning electron microscopy (SEM)), the other electrical characteristics with using Prova tool and home-set electrical measurement system as well as transmittance and reflection parameters measurement system, could provide a suitable ENG for future of the optoelectronic and electromagnetic devices.

© 2026 The Author(s). Innovations in Materials: Current &amp; Future, published by Semnan University Press.

This is an open access article under the CC-BY-NC 4.0 license. (<https://creativecommons.org/licenses/by-nc/4.0/>)**1. Introduction**

Since the possibility of synthesizing materials with a negative refractive index has been reported, it has been very difficult to find a metamaterial with excellent characteristics due to the synthesis of a very regular framework, and not many works were reported in this field. When the researchers realized that by introducing metal particles such as silver nano-particles in the dielectric matrix [1] which has an amorphous and random structure (such as aluminum oxide dielectric matrix), a metamaterial with negative permittivity ( $\epsilon$ ) and permeability ( $\mu$ ) can be synthesized, the study of these material applications has been increased remarkably [2-10]. However,  $\epsilon$ ,  $\mu$  parameters can

both have positive ( $\epsilon > 0$ ,  $\mu > 0$ ) or negative values ( $\epsilon < 0$ ,  $\mu < 0$ ), and one of them can have positive values and the other can have negative values ( $\epsilon > 0$ ,  $\mu < 0$ ), or ( $\epsilon < 0$ ,  $\mu > 0$ ), which define four classifications or four regions. Normal materials have both positive parameters ( $\epsilon > 0$ ,  $\mu > 0$ ). Metamaterials that have both negative parameters ( $\epsilon < 0$ ,  $\mu < 0$ ) are known as double negative metamaterials. But if one of these parameters is negative ( $\epsilon > 0$ ,  $\mu < 0$ ), or ( $\epsilon < 0$ ,  $\mu > 0$ ), it is known as single negative or left-hand material. Here, an attempt has been made to only synthesize and study materials with epsilon or negative permittivity ( $\epsilon < 0$ ), where our previous work [3,4]

\* Corresponding author.

E-mail address: [a.bahari@umz.ac.ir](mailto:a.bahari@umz.ac.ir)**Cite this article as:**Bahari, A. and Farhadi, A., 2026. Epsilon- negative (ENG) composites characteristics at GHz frequency. *Innovations in Materials: Current & Future*, 1(1), pp. 46-50.<https://doi.org/10.111111/IMCF.2024.39315.2050>

showed ( $\mu > 0$ ). This material is examined at high frequencies up to 12 terahertz (GHz).

In this regard, some key parameters should be considered. From scattering matrix, two parameters that reflection coefficient ( $S_{11}$ ) and transmission coefficient ( $S_{21}$ ) should be measured, and of course the characteristics of materials are strongly dependent on frequency changes, so that they exhibit unusual behavior at frequencies in the GHz range. Here, the real ( $\epsilon_{\text{Real}}$  or  $\epsilon_r$ ) and imaginary or complex permittivity ( $\epsilon_{\text{Imaginary}}$  or  $\epsilon_i$ ), and scattering (S) parameters ( $S_{11}$  and  $S_{21}$ ) are measured as a function of frequency with using Nicolson-Ross-Weir (NRW) method [8-14].

To construct such this structure, ferrite-based materials, especially garnet (Yttrium iron garnet; YIG, named FYIG; ferrite yttrium iron copper garnet; FYICG, with different lithium (0.02 gr, 0.2 gr, 0.4 gr), as incoming nano crystallites mixed into the FYICG matrix have been investigated. It is seen that filling factor (the the ratio of concentration of incoming of metallic (here, Li) nano particles - concentration of matrix (here, FYICG) particles play key role and should be controlled [15,16]. This factor not only influence the occupied/ unoccupied sites for incoming crystallites (nano particles), but the negative electrical permittivity at 8-12 GHz frequencies can change polarization, exchange particles potential and self- energy, vertex function and resistivity.

In the present work, devices with negative permittivity of nano-particles with stoichiometry ratio 5:3 of ( $\text{Fe}_2\text{O}_3 + \text{Y}_2\text{O}_3$ ) powder (FYIG, synthesized at room temperature, and atmosphere condition) +0.5gr Cu (FYICG, synthesized at room temperature, and atmosphere condition), Li (LL: 0.02gr, T=650°C)/FYICG, Li(M:0.2gr, T=1000°C)/FYICG, Li (HL: 0.02gr, T=1250°C)/FYICG, Li(HH: 0.2gr, T=1250°C)/FYICG are prepared using the in situ method. To investigate the 6 present sample (FYIG, FYICG, Li(LL)/FYICG, Li(M)/FYICG, Li(HL)/FYICG, Li(HH)/FYICG characteristics, some relevant techniques such as X-Ray diffraction patterns XRD, scanning electron microscopy (SEM) and home -set electrical system, the Mega-TEC, DC power supply (MIP-300SD) tool, and Prova tool have been applied, in where all samples show a single cubic crystal structure with the general formula  $\text{A}_3\text{B}_5\text{O}_{12}$ . The permittivity ( $\epsilon$ ), electrical transfer, cut-off frequency, and S-parameter show all electrical, dielectric and optical parameters are so sensitive to variations in frequency of applied field.

The dielectric properties with 0.2gr, T=1000°C Li is dominated by conduction and polarization, in where the  $S_{11}$ ,  $S_{21}$ , or  $\epsilon_r$ , or  $\epsilon_i$  of Li(M)/FYICG sample results indicate that sample Li(M)/FYICG with higher  $S_{11}$ ,  $S_{21}$  and negative epsilon ( $\epsilon < 0$ ,  $|\epsilon| \geq 1$ ) a in some frequencies of the applied field compared

to the other 5 samples of the present work can act as a very good amplifier. Therefore, Li(M)/FYICG with a tunable negative dielectric constant have great potential in optoelectronic, electromagnetic damping, shielding, and antenna fields.

## 2. Experimental procedure and details

The more details of synthesis procedure can be found in our recent published works [3-7]. Here according to the relationship of chemical reactions below,



To add, for example, 10% of copper nanoparticles (here 0.5 gr copper), 5 grams of garnet (FYIG; yttrium oxide ( $\text{Y}_2\text{O}_3$ ) -iron oxide ( $\text{Fe}_2\text{O}_3$ ) 3:5 stoichiometry ratio) are needed. Then, 0.02, 0.2 gr of lithium nanoparticles is added to a container containing FYIG and copper oxide (CuO), named FYICG sample. Also, samples have then entered a container of 99.999% pure ethanol and then become powders or nano crystallites with using ball milling for 10 hours and finally centrifuged and dried in a vacuum dried at 80°C. The resulting dried powders are pressed into rectangular bars measuring  $22.8 \times 10.1 \times 3 \text{ mm}^3$  under 30 MPa pressure, sintered at  $T=1000^\circ\text{C}$  for one hour (1h) and placed in a tube furnace filled with 99.9% pure hydrogen gas at 500°C for 3h. Maximum 10 grams of the powder were used for measuring scattering parameters with Vector Network Analyzer (VNA) conducted over the 80-120 GHz frequency range. Concurrently, including those outlined above, 6 Al/FYIG-Based/Al capacitors with a distance of  $L=10 \text{ mm}$  and  $10 \text{ mm}^2$  surface area are fabricated. After applying electric field, say voltages to Al electrodes, the output currents are measured with home -set electrical system, the Mega-TEC, DC power supply (MIP-300SD) and Prova tool, where, the transconductance ( $g_m$ ), the current- gain cutoff frequency ( $f_T$ ) and admittance ( $Y_{Ad}$ ) of the samples can be estimated by flowing Eq. (2) [8];

$$g_m = \frac{\partial I}{\partial V}, f_T = \frac{g_m}{2\pi C_i}, Y_{Ad} = \frac{I_{DS}}{\sqrt{g_m}} \quad (2)$$

In where the capacitance per unit area of FYIG, FYICG, Li(LL)/FYICG, Li(LL)/FYICG, Li(LL)/FYICG, Li(LL)/FYICG, is 25, Cutoff- frequency and admittance of present samples are shown in Fig. (1) with different values, in that Li(M) has better  $g_m$ ,  $f_T$ , and admittance in comparison to those for other present samples. In Fig. (1), three curves related to ( $g_m$ ) transconductance, cut-off frequency ( $f_T$ ) and admittance (Y) with applied voltage of 0-10 V on the aluminum capacitor/current work material/aluminum (Al/Ferrite-based materials/Al device) with an area of  $10 \text{ mm}^2$  and  $d= 10 \text{ mm}$ , are shown. It is evident in these curves that by applying voltage to

the capacitor, the  $g_m$ ,  $f_r$ , and  $Y$  parameters changed as Boltzmann- function or Sigmoid -function. It (for Li(HH)/FYICG) could be due to the effect of heat on this sample, which is 1250°C, (The  $Y$  after applying  $V > 9$  V, shows an increasing exponential growth.

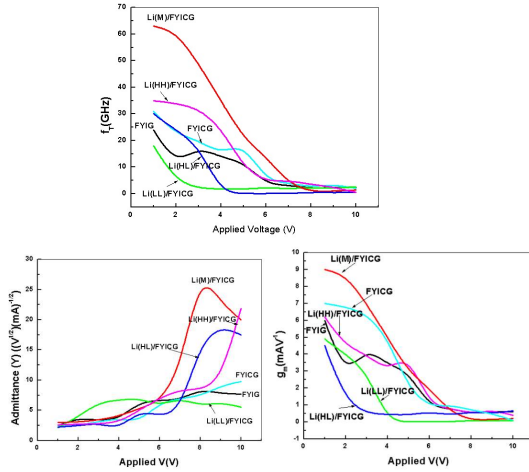


Fig. 1. Transconductance ( $g_m$ ), Cutoff frequency ( $f_r$ ), Admittance ( $Y_{Ad}$ ) of the present samples.

When the cut-off frequency of the present samples showed different values, it causes to study the frequency dependent of the electrical and dielectric characters of the samples. For this reason, electrical permittivity ( $\epsilon$ ) was measured with two real,  $\epsilon_r$  and imaginary,  $\epsilon_i$  components of the  $\epsilon$ , which represent electrical and conductivity, respectively. Also, from Fig. (2);  $\tan \phi = \epsilon_i / \epsilon_r$ , gives the phase tangent (denoting energy loss). If  $\tan \phi < 1$ , then  $\epsilon_i < \epsilon_r$ , meaning that the dielectric character of the sample is dominant, whilst if  $\tan \phi > 1$ , then  $\epsilon_i > \epsilon_r$ , meaning that it expresses the conductivity character of the sample [3,4, 7, 8]. As shown in Fig.2, Li(M)/FYICG and Li(HH)/FYICG have kept their dielectric character, but other samples have conductivity to dielectric and/or dielectric to conductivity characters. The dielectric constant ( $\epsilon_r$ ) can be found with considering the relation of capacitor capacity, which is:

$$C_{\text{Gate dielectric}} = \epsilon_r \epsilon_0 \frac{A}{d_{\text{Gate dielectric}}} \rightarrow$$

$$\epsilon_r = C_i \frac{d_{\text{Gate dielectric}}}{\epsilon_0} \quad (3)$$

$$X_C = \frac{1}{\omega C_{\text{Gate dielectric}}} \quad (4)$$

On the other hand; But since the imaginary component known as dielectric loss ( $\epsilon_i$ ) has a relationship with impedance. Impedance, which has the real component of electrical resistance and the imaginary component of the difference  $X_L = L\omega$

related to the inductor from  $X_C = 1/C\omega$  related to the resistance of the capacitor, can be seen in [8-10]. Here, only the resistance related to the capacitor, which is  $X_C$ , is involved and is discussed, because this resistance gives conductance ( $G$ ), which is:

$$\frac{\partial D}{\partial t} = \frac{\partial E}{\partial t} + 4\pi J, E(t) = E_0 e^{-i\omega t}$$

$$-i\omega \epsilon E = -i\omega E + 4\pi \sigma E \rightarrow$$

$$\epsilon_i = \frac{4\pi}{\omega} \text{Re}(\sigma) = \frac{1}{\epsilon_0 \omega} G \equiv \frac{d_{\text{Gate dielectric}}}{\omega A \epsilon_0} G$$

$$\epsilon_i = \frac{d_{\text{Gate dielectric}}}{\omega A \epsilon_0} G \quad (5)$$

In our previous works [3, 4, 6] for other incoming metallic nano crystallites into Ferrite- and dielectric- based materials, conclusions show that the electrical AC conductivity ( $\sigma_{AC}$ ) and also ( $\sigma_{AC} - \sigma_{DC}$ ) where  $\sigma_{DC}$  is direct exhibit a non-linear frequencies dependence, whilst if the material contains an ideal double dipole, this relationship becomes linear, i.e.;  $\sigma_{AC} - \sigma_{DC} = A\omega$ . The reason could be due this fact that always the density of traps and other defect factors like creation and annihilation states can influence to polarization and annihilation states can influence to polarization and bulk plasmon, in particularly many-body interactions, meaning that the state of the structure of the material is not ideal [11-14], or;

$$\sigma_{AC} - \sigma_{DC} = A\omega^n, 0 < n < 1 \quad (4)$$

And also;

$$\sigma_{AC} = \omega \epsilon_0 \epsilon_i, \sigma_{DC} = \sum_i N_i \mu_{\text{eff}} q_i \quad (5)$$

Where  $N_i$  is charge carrier density. These issues will be discussed in details in the next section.

One of the main challenges in carrier mobility, transconductance, cut-off frequency investigation is sample surface morphology, in that surface with lower roughness yields to more current density flux [4]. Figure 2 shows the surface morphology of FYICG, Li(HL)/FYICG, Li(M)/FYICG and Li(HH)/FYICG samples, using FESEM (Field effect scanning electron microscopy) technique. Microscopic images taken from the surface of FYICG, Li(HL)/FYICG, Li(M)/FYICG and Li(HH)/FYICG show that sample Li(M)/FYICG has a brighter surface and a more uniform and more integrated surface than those of the other samples (FYICG, Li(HL)/FYICG, and Li(HH)/FYICG) surfaces.

The obtained results indicated that higher carrier mobility and higher output current density can increase in the speed of the electric charge carrier for a surface with less roughness can ultimately yield to a higher current density. Of course, the

properties of the surface of the sample are different from the properties of its bulk, and they can therefore show different conductivity and dielectric properties.

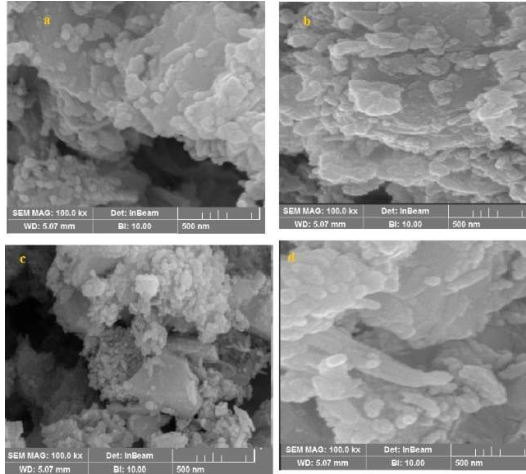


Fig. 2. FESEM images of (a) FYICG; (b) Li(HL)/FYICG; (c) Li(M)/FYICG (d) Li(HH)/FYICG samples.

### 3. Result and discussion

After analyzing the SEM images, since the optoelectronic, electromagnetic such as antenna's impedance bandwidth is mainly affected by its return loss and also cut frequency depend of the present sample properties with different transconductance and admittance behaviors, the dielectric function, scattering and/or permittivity (reflection or the return loss,  $S_{11}$  and transmittance,  $S_{21}$  coefficients) parameters are studied at high frequency (80-120 GHz) and using Nicolson Ross weir method [11-15]. These parameters are found by Nicolson Ross weir method [9-12] as follow;

$$\Gamma = k \pm \sqrt{k^2 - 1} \quad (6)$$

where,

$$k = \frac{\{S_{11}^2(\omega) - S_{21}^2(\omega)\} + 1}{2S_{11}(\omega)}$$

$$T = \frac{\{S_{11}(\omega) + S_{21}(\omega)\} - \Gamma}{1 - \{S_{11}(\omega) + S_{21}(\omega)\}\Gamma}$$

$$\epsilon_{ratio} = \Lambda \frac{1 - \Gamma}{1 + \Gamma} (\lambda_0^3 \lambda_c) \frac{(\Lambda^{-2} + \lambda_c^{-2})}{\sqrt{\lambda_c^2 - \lambda_0^2}}$$

$$\frac{1}{\Lambda^2} = - \left[ \frac{1}{2\pi d} \ln \left( \frac{1}{T} \right) \right]^2 \quad (7)$$

where  $\Gamma$  is the reflection coefficient at intrinsic impedance in air / present samples interface, in that the length of material(d) is infinite.

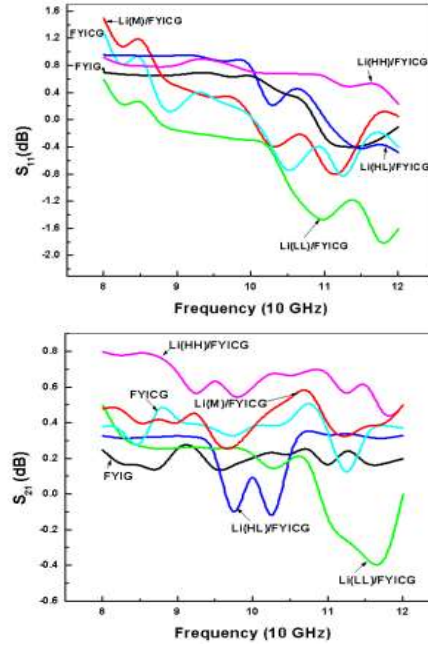


Fig. 3. The  $S_{11}$  and  $S_{21}$  parameters of (a) FYICG; (b) Li(HL)/FYICG; (c) Li(HH)/FYICG (d) Li(M)/FYICG samples in the 8-12 GHz frequency range.

$T$  is the transmission coefficient in the materials,  $\epsilon_{ratio}$  relative permittivity of material,  $\lambda_0$ , and  $\lambda_c$  is the free space and cut-off wavelength of the wave guide, respectively [14-18]. The obtained measurement results based on Eqs. (6,7) shown in Figs. (3-6) demonstrated different dielectric and conductivity characteristics of the present samples. Figure (3) shows the curves of  $S_{11}$  and  $S_{21}$  parameters of the present samples. It reveals how  $S_{11}$  and  $S_{21}$  parameters change with frequency changes in the range of 80-120 GHz.

The higher  $S_{11}$  and a lower  $S_{21}$  for a sample means that sample can perform better in the faster shift of the operating frequency to the resonance frequency, which this characteristic can increase the efficiency of the device, as an amplifier. As shown in Figs. (3-6), it is clear that the Li(M)/FYICG sample is the most desirable sample among the samples of the present work.

Figures (4-6) display the frequency-dependent permittivity curves of FYICG, Li(HL)/FYICG, Li(HH)/FYICG, Li(M)/FYICG samples in the 8-12 GHz frequency range. These parameters are used to evaluate the dielectric and conductivity characteristics of the present samples in where imaginary part of permittivity ( $\epsilon_i$ ) indicates the loss properties of materials that absorb electromagnetic waves. Real part of the permittivity ( $\epsilon_r$ ) indicates the ability to store electromagnetic energy, whereas as stated above, imaginary permittivity ( $\epsilon_i$ ) relate to energy dissipation and magnetic loss, respectively. The plot in Figs. (4,6) and data outlined in Table (1), show that the real parts of the permittivity for the FYIG, Li(HH)/FYICG, and especially Li(M)/FYICG samples are negative and covered most of the resonance band.

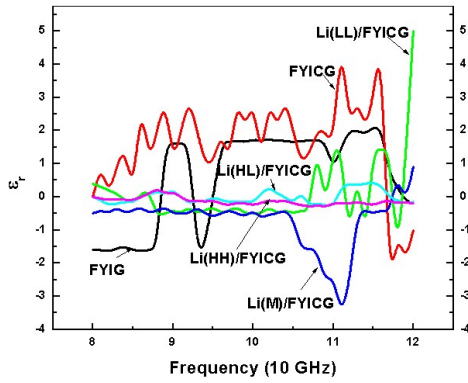


Fig. 4. Real component  $\epsilon_r$  ( $\epsilon_{Real}$ ) of the permittivity spectra of the present samples.

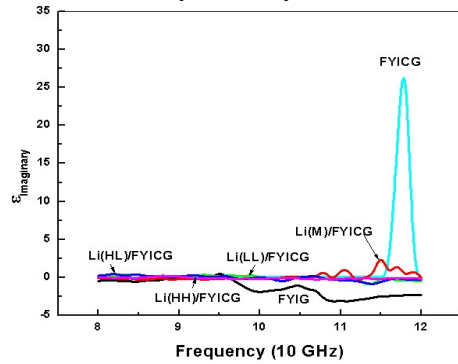


Fig. 5. Imaginary component  $\epsilon_i$  ( $\epsilon_{Imaginary}$ ) of the permittivity curves of the present samples.

The morphology of the sample surface, plasmon and grain boundaries through the exchange electrical charge carriers, interaction of Li, iron, and yttrium atoms and in particularly hopping electrical charge carriers like electrons and polaron can create polarization at boundary locations due to the high resistance of the grain boundaries [22-24]. The conductivity of FYICG is high at  $f < 11.7$  GHz frequencies, due to maybe their electron exchange and electrical responsivity (Exchange  $Cu^{2+}$  ions) and the interconnected of Cu atoms can form a conductive network, leading to an increase in conductivity. Both permittivity (real and imaginary components) of Li(M)/FYICG demonstrated that this sample has better dielectric polarization and relaxation effects. Figs. (4,5) show the dielectric polarization properties are improved by maybe due to the back-bonds, surface plasmon and inter-band transitions as incoming particles into the FYICG matrix. These issues could force the free charges to be build-in at the Al/ Li(M)/FYICG interface layer, which cause two-phase conductive performance when the conductive phase is distributed in the insulating matrix to form composite materials.

Table (1). ENG of the samples.

Sample	FYIG/	Li(HH)/	Li(M)/	Li(M)/
		FYICG	FYICG	FYICG
ENG	-1.5	-0.1 to -0.3	-0.1 to -0.3	-1 to -3.3
	$f = 80-90$ GHz	$f = 80-120$ GHz	$f = 80-105$ GHz	$f = 105-113$ GHz

Moreover, in Figs. (4,5) some dominated peaks with minimum and maximum values for some lines, indicating a resonance phenomenon such as Fano resonance peak [2-7].

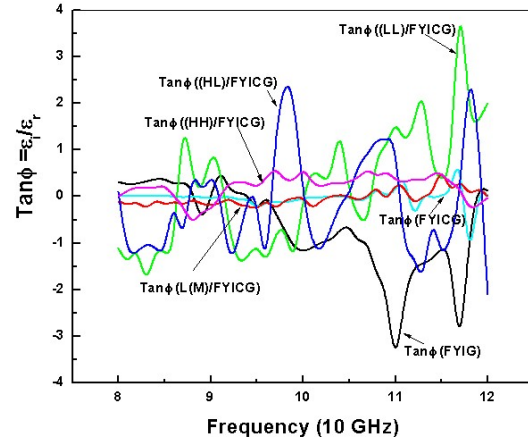


Fig. 6:  $Tan \phi = \epsilon_i / \epsilon_r$ , gives the phase tangent of the present samples.

In Fig. (6), it can be seen that the  $Tan(\phi)$  of sample FYIG has little changes up to the frequency of 9 terahertz (GHz), and after 9 GHz,  $Tan(\phi)$  shows large changes in some frequencies, but these changes of the  $Tan(\phi)$  up to the frequency of 10.5 GHz are smaller than 1, which indicates that the dielectric characteristic of this sample is dominant over its conductivity characteristic. The  $Tan(\phi)$  of FYIG sample at the frequency of 11 GHz shows a very high negative value, -3, which is clear from [1-9] that when  $Tan(\phi) > 1$ , it means that the conductivity characteristic is dominant over the dielectric characteristic.

Polarization (p), total potential of material (V), as discussed in details in [1], should be taken into account for dielectric response to applied field, so that;

$$\epsilon = 1 - VP \quad (8)$$

From the negative refractive ( $\epsilon < 0$ ) properties ( $VP > 1$ ), called epsilon-negative because of its negative permittivity (ENG), [10-15], and studied with applying above equations and the Nicolson-Ross-Weir (NRW) method as a standard method [3, 9,16], the measurement of imaginary part of the permittivity has become increasingly important with the increased use of the RF and microwave spectrum, particularly in polymer composites,

engineered materials such as compound layer dielectrics [10] applications.

In the present work, increasing the concentration of lithium crystallites in FYIC matrix, can cause more polarization ( $p$ ) and  $V$ , in where at higher frequency,  $VP > 1$ , and  $\epsilon < 0$  due to more conduction electrons for a negative dielectric constant.

In fact, yttrium iron garnet (YIG) which is a ferrite material with excellent magneto-electric and magneto properties, when doped with copper ions, show a conductive role and thus a good candidate for high frequency applications [13]. Some people [1,6,13-16] have reported that YIG doped with zinc, cobalt, and nickel and so on, could show tunable negative electromagnetic parameters as well, but these composites reached the percolated states, and thus lose their stability [3, 21, 22].

The main goal of the present work is to study the ENG behaviors of Li/FYICG nano-composites with various concentrations of Lithium as a conductive network, synthesized by in situ route via experimental descriptions of structural and scattering parameter, and imaginary permittivity in Terahertz regime (here 8-12 GHz) with the help of VNA from Agilent Technologies, model HP 8510 give finally S-parameters ( $S_{11}$  and  $S_{21}$ ) values.

#### 4. Conclusions

In summary, the FYIG, FYICG nanocomposites with different Li contents (0.02 gr, 0.2 gr) are prepared by in situ method at room temperature and 650, 1000 and 1250°C, and then their dielectric, conductivity and electromagnetic characteristics have been investigated in the frequency ranges of 8–12 GHz. The incoming Li particles into the FYICG matrix can affect the nanostructural properties of the present samples so that, the accumulation of Li nano crystallites (Particles) in the present ferrite-based materials and Al interface can form a conductive (dielectric) network to increase (decrease) conductivity, in which conductive (dielectric) network may generate negative permittivity in Terahertz frequency regime. Left-hand and/or single negative material could be synthesized by adjusting filling factor (Li nano crystallite concentration or numbers versus FYICG matrix concentration) and synthesize conditions and composition of the composites, which Single negative materials (SNMs) have shown a great significance on the development of optoelectronic, electromagnetic, antenna and invisible coating devices.

#### Conflict of Interest Statement

The authors declare that there are no conflicts of interest regarding the publication of this paper.

#### Data Availability Statement

The datasets generated for and/or analyzed during the current study are available from the corresponding author on reasonable request. Further inquiries can be directed to the corresponding author.

#### Authors Contribution Statement

Ali Bahari: Supervision, Conceptualization, Resources, Writing - Review & Editing, Methodology; Validation. Abbas Farhadi: Investigation; Validation; Visualization.

#### References

- [1] Inkson, J. C., 1984. Many-body theory of solids, ISBN 978-1-4757-0226-2 (eBook), 1984 Plenum Press, New York.
- [2] Nazri, A., 2019. Adsorption potential of magnetite nanoparticles for Lithium removal from aqueous solution, *Nature*, 2, PP. 3-15.
- [3] Abouk, A., Bahari, A. and Gholipur, R., 2023. Synthesis and characterization of Cu/YIG nanoparticles- Terahertz material, *Optical materials*, 142, PP.113992-99.
- [4] Bahari, A., 2024. Eco-friendly water induced lithium oxide/ polyethyleneimine ethoxylated as a possible gate dielectric of the organic field effect transistor, *Journal of Materials Science: Materials in Electronics*, 35, PP. 1709-1716.
- [5] Gholipur, R. and Bahari, A., 2015. Random nanocomposites as metamaterials: preparation and investigations at microwave region, *Optical Materials*, 50, PP. 175-183.
- [6] Khorshidi, Z., Gholipur, R., and Bahari, A., 2016. Studies on properties of Ag/Co<sub>0.05</sub>Ti<sub>0.95</sub>O<sub>2</sub> random nano composite as metamaterials, *Optical Materials*, 60, PP. 418-421.
- [7] Delkhosh, F., Bahari, A., Gholipur, R., 2025. Synthesis and investigation of electro - magnetic properties and refractive index in terahertz frequencies for nanoparticle-based metamaterials with Ni doped Cu/YIG, *Optical Materials*, 161, PP. 116765-775.
- [8] Sun, K., 2015. Random Lithium/yttrium iron garnet composites with tunable negative electromagnetic parameters prepared by in situ synthesis, *RSC Advances*, 5 (75), PP. 61155-61160.
- [9] Niguma, R., Wada, K., and Okamoto, K., 2024. Novel Plasmonic Metamaterials Based on Metal Nano-Hemispheres and Metal-Dielectric Composites, *Photonics*, 11 (4), PP. 356-364.

- [10] Shahbazi, M., Bahari, A., and Ghasemi, Sh., 2016. Structural and frequency-dependent dielectric properties of PVP-SiO<sub>2</sub>-TMSPM hybrid thin films, *Organic Elect.*, 32, PP. 100-108.
- [11] Susek, W., Dukata, A., and Pomaranska, P. , 2023. A Formal Approach to the Extraction of Permittivity and Permeability of Isotropic and Anisotropic Media Using the TM<sub>11</sub> Mode in Rectangular Waveguides, *Electronics*, 12 (13) , PP. 2899-2906.
- [12] E. Sheta, P. Choudhury, and A.-B. M. Ibrahim, Polarization-insensitive ultra-wideband metamaterial absorber comprising different forms of ZrN structures at the metasurface, *Optical Materials*, 133 (2022) 112990-97.
- [13] Xie, P., 2022. Recent advances in radio-frequency negative dielectric metamaterials by designing heterogeneous composites, *Advanced Composites and Hybrid Materials*, 5 (2), PP. 679-695.
- [14] Gholipur, R., and Bahari, A., 2017. Tun-ability of negative permittivity and permeability of Ag/Zr<sub>0.9</sub>Ni<sub>0.10</sub>Y nanocomposites with morphology, *Electronic Materials Letters*, 13 , PP. 179-183.
- [15] Pianelli, P., 2022. Active control of dielectric singularities in indium-tin-oxides hyperbolic metamaterials. *Science Report*, 12, PP. 16961-73.
- [16] Wu, H. , 2023. Microstructure and gyromagnet properties of In-substituted YIG ferrite prepared by sol-gel method, *Journal of Materials Science: Materials in Electronics*, 34 ( 9), PP. 823-831.
- [17] Cheng, Ch., Liu, Y., Ma, R., and Fan, R., 2022. Nickel/yttrium iron garnet metacomposites with adjustable negative permittivity behavior toward electromagnetic shielding application, *Composites Part A: Applied Science and Manufacturing*, 155, PP. 106842-51.
- [18] Mohaidat, Q. I. , Lataifeh, M. , Hamasha, K., Mahmood, S. H., Bsoul, I. , and . Awawdeh, M, 2018. The structural and the magnetic properties of aluminum substituted yttrium iron garnet, *Materials Research*, 21, PP. 21-31.
- [19] Maeda, S. , Osaka, N. , Niguma, R., Matsuyama T., and Okamoto, K., 2023. Plasmonic Metamaterial Ag Nanostructures on a Mirror for Colorimetric Sensing, *Nanomaterials*, 13, PP. 1650-63.
- [20] Li, W., et al., 2023. Improved permeability and decreased core loss of iron-based soft magnetic composites with YIG ferrite insulating layer, *Journal of Alloys and Compounds*, 937, PP. 168285- 93.
- [21] Gholipur, R.. and Bahari, A., 2017. Alignment of Ag nanoparticles by an external electric field proposed for metamaterial applications, *Current Applied Physics*, 17(7), PP. 989-998.
- [22] Moreau, A., et al., 2012. Controlled-reflectance surfaces with film-coupled colloidal nanoantennas, *Nature*, 492 (7) , PP. 86-89.